QUANTIFYING FAULT NETWORKS ON ALBA PATERA, MARS. D. Y. Wyrick[1], D. A. Ferrill[1], A. P. Morris[2], D. W. Sims[1], and N. M. Franklin[1], [1]CNWRA, Southwest Research Institute® (6220 Culebra Road, San Antonio, TX 78238, USA, dwyrick@swri.org), [2]Department of Earth and Environmental Science, University of Texas at San Antonio (6900 N. Loop 1604 W., San Antonio, TX 78249)

Introduction: Modeling of a martian hydrosphere has relied primarily on regional to global scale models based on morphological, hydraulic or thermal conditions [1,2] to determine paleo groundwater flow and potential ground ice storage. Although the influence of structural features on groundwater has been noted [1,2], to date hydrological models have not incorporated the influence of structural features such as faults and fractures. On Earth, fault systems have been demonstrated to impart heterogenous and anisotropic permeability to aquifer systems [3] and likely play a similar role on Mars. Quantifying the extent and degree of fault network connectivity will provide key constraints for hydrological models. The availability, resolution, and essentially two-dimensional nature of surface data limits the types of analyses that can be performed to characterize subsurface martian geology. Conversely, the excellent preservation of fault scarps due to low erosion rates on Mars lends itself to detailed analysis. With the aid of high resolution imagery such as MOC and THEMIS, it is now possible to incorporate structural analyses of fault systems to evaluate their potential influence on permeability in the martian crust.

Networks of normal faults generally evolve from systems of unconnected (isolated) fault ruptures, to poorly connected networks formed by linkage of propagating fault segments, producing corrugated faults, to strongly interconnected fault networks with isolated fault blocks. This evolution tends to progress with increasing duration or magnitude of extension [4]. The interconnectedness of faults and/or fault blocks is important for considerations of earthquake magnitude [5] and the development of permeability anisotropy and discrete flow pathways [3].

In this paper, we use newly developed approaches (see 4, 6, 7) that can readily be applied to martian fault network maps to perform direct measurements of the interconnectedness of the fault network, interconnectedness of fault blocks, and fault density. These analytical tools yield insight into permeability architecture that could aid modeling and analysis of fluid movement through a faulted aquifer. These approaches have the advantage that they can be applied to map view data sets such as the remotely sensed data (e.g., photographic, digital elevation data) from planetary surfaces, thus providing a new tool for analysis of the extensive array of available data sets. We then apply these approaches to characterization of faults on Alba Patera, Mars, for which recent high-resolution THEMIS visual spectrum imagery is available. Alba Patera has complex fault systems on its flanks that provide good examples of the utility of fault network analysis. This approach, when applied to martian data sets, can provide quantitative data on permeability relevant to groundwater or gas (e.g., methane), storage of ice and locations of potential sites of mineralization.

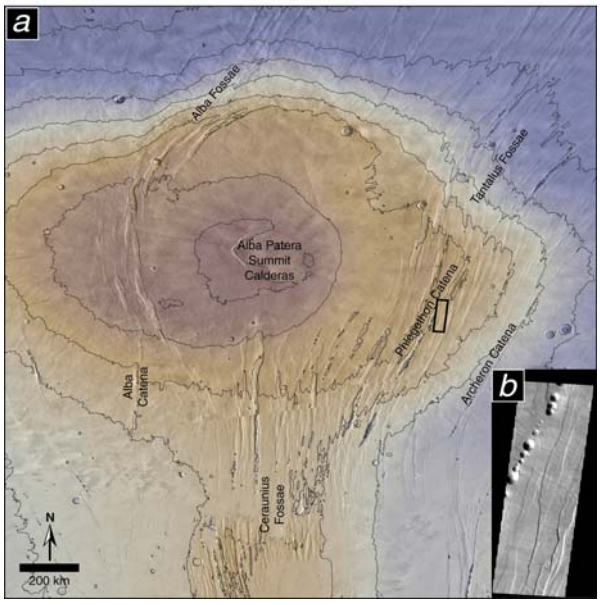

Figure 1: (a) Overview image of Alba Patera, Mars, showing major horst and graben features (fossae) and pit crater chains (catena). Overlay of MOLA topography data on Viking Mosaic (MDIM 2.1). Red indicates regional highs; blue indicates lows. (b) THEMIS image V01202006 located in Phlegethon Catena region.

Application to faulting of Alba Patera, Mars:

Alba Patera is a large, low-relief shield volcano located in the northern region of the Tharsis uplift on Mars (Fig. 1). Alba Patera has a long history of tectonic activity dating from the Noachian to the Late Amazonian [8]. This volcano has associated normal faults that strike tangential to the volcano on the eastern side and tangential to circumferential on the west/northwest flanks. Normal faulting in the Alba Patera region is characterized by horst and graben formation (fossae) and pit crater chains (catena). The

southeastern area represents the older Hesperian age NNE-SSW trending Tantalus Fossae formation [8].

The fault system on the southeast flank of Alba Patera exhibits many en echelon arrays, curved fault tips and relay ramp features indicating fault linkage and propagation of normal faults (Fig. 2). A few large, well-developed faults extend across the region, but most deformation is accommodated by numerous faults with relatively small displacement (~ 40 m). Although not mapped as a fault, the pit chain crossing the northern subarea likely represents a fault or network of faults at depth [9,10]. The consistent NNE-SSW strike of faults conforms to the radial (to the Tharsis uplift) faulting of the Tantalus Fossae during the Hesperian [11].

The three subareas of the southeastern region of Alba Patera display a consistent faulting style. A dominant NNE-SSW fault orientation is observed throughout the mapped area. Rock mass connectivity plots (Fig. 2b) for this region are consistent in both size and orientation, with the rock mass connectivity plots yielding smaller size distributions than the fault network connectivity plots (Fig. 2c). The northernmost subarea has a slightly higher rock mass connectivity than the other two subareas, reflecting the relatively large unfaulted region in the southwestern quadrant of the subarea and the pit chain (catena) transecting the area of interest. Fault density maps illustrate the areal variation across the three sampled areas. This is most apparent in the northern area where fault densities are low in the areas occupied by the catena.

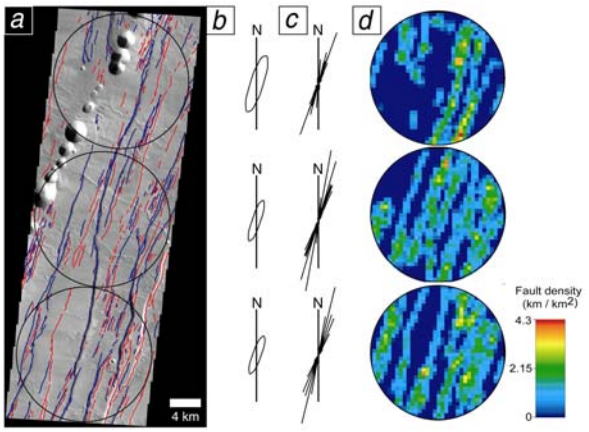

Figure 2: Fault network analysis of Tantalus Fossae region: (a) fault map of footwall traces, (b) rock mass connectivity, (c) fault network connectivity plots of mapped faults, (d) fault density maps based on total fault trace length per unit area.

Discussion:

The southeastern Alba Patera fault system (Tantalus Fossae) likely represents the Hesperian age faulting radial to the Tharsis rise. Concentric faulting west of the study area crosscuts the NNE-SSW trend of the Tantalus Fossae. However, pit chains following the orientation of the older system, e.g., the Phlegethon Catena (Figs. 1 and 2), clearly crosscut the younger concentric faulting of the Amazonian age. The reactivation of the NNE-SSW trend is relatively young and displacements are small. These faults likely have a dilatant geometry at depth and thus have generated pit chains [9, 10].

Conclusions:

Fault connectivity, rock mass connectivity, and fault density analysis provide quantitative means to determine potential permeability anisotropy and preferential flowpaths. The characteristics of fault network connectivity can be used to quantitatively and qualitatively describe a fault system. The degree to which faults are connected influences the flow of groundwater. If faults act as barriers to groundwater flow, then the size, extent and orientation of the rock mass connectivity plot can be used to describe the average uninterrupted flow path within inter-fault blocks. Conversely, faults may act as conduits to flow such as is indicated by the pit chain development over a dilational fault. In this case, the fault length and orientation, combined with analysis of fault linkage can be used to determine the average uninterrupted flow along faults. Current interpretations of the distribution of martian groundwater systems should incorporate the influence of faults on flowpaths. These fault network characterizations can be applied to remotely sensed data, either terrestrial or planetary, to assist in evaluating permeability characteristics.

References:

[1] Carr, M. H. (1996) *Water on Mars*. Oxford Univ. Press, New York. [2] Clifford, S. M. and Parker, T. J. (2001) *Icarus*, 154, 40-79. [3] Ferrill, D. A. et al. (1999) *GSA Today*, 9(5), 1-8. [4] Sims, D. W. et al. (*in press*) in *Faults, fluid flow, and petroleum traps*, AAPG Memoir. [5] Ferrill, D. A. et al. (1999) *J. Structural Geology*, 21, 1027-1038. [6] Waiting, D. J. et al. (2003) *Proc. of 10th Int. High Level Radioactive Waste Management Conf.* [7] Morris, A. P. et al. (2004) *J. Structural Geology*, 26, 1707-1725. [8] Cailleau, B. et al. (2003) *JGR, 108*(E12). [9] Ferrill, D. A. et al. (2004) *GSA Today 14* (10), 4-12. [10] Wyrick D. Y. et al. (2004) *JGR* 109, E06005. [11] Tanaka, K. L. (1990) *Proc. of 20th Lunar Science Conf.*, 515-523.